J|A|C|S
ARTICLES
Published on Web 04/11/2007

Hierarchical Assembly of Model Cell Surfaces: Synthesis of Mucin Mimetic Polymers and Their Display on Supported Bilayers

David Rabuka,[†] Raghuveer Parthasarathy,[†] Goo Soo Lee,[†,||] Xing Chen,[†] Jay T. Groves,[†,||] and Carolyn R. Bertozzi*[,†,‡,§,||,⊥]

Contribution from the Departments of Chemistry, Molecular and Cell Biology, and Howard Hughes Medical Institute, University of California, and Materials Sciences Division and The Molecular Foundry, Lawrence Berkeley National Laboratory, Berkeley, California 94720

Received November 1, 2006; E-mail: crb@berkeley.edu

Abstract: Molecular level analysis of cell-surface phenomena could benefit from model systems comprising structurally defined components. Here we present the first step toward bottom-up assembly of model cell surfaces—the synthesis of mucin mimetics and their incorporation into artificial membranes. Natural mucins are densely glycosylated O-linked glycoproteins that serve numerous functions on cell surfaces. Their large size and extensive glycosylation makes the synthesis of these biopolymers impractical. We designed synthetically tractable glycosylated polymers that possess rodlike extended conformations similar to natural mucins. The glycosylated polymers were end-functionalized with lipid groups and embedded into supported lipid bilayers where they interact with protein receptors in a structure-dependent manner. Furthermore, their dynamic behavior in synthetic membranes mirrored that of natural biomolecules. This system provides a unique framework with which to study the behavior of mucin-like macromolecules in a controlled, cell surface-mimetic environment.

Introduction

Cell-surface phenomena have been largely refractory to molecular level analysis due to the highly complex and dynamic nature of the cell membrane and its associated biopolymers. Efforts to understand how cell-surface molecules guide interactions with other cells and extracellular matrix components could benefit tremendously from structurally defined synthetic model systems. The bottom-up fabrication of such systems begins with the identification of prevalent cell-surface-associated molecules and the generation of membrane-bound mimetics that retain biological function.

Mucins are part of the cell-surface glycoprotein repertoire modulating critical cell−cell interactions.[1] They are characterized by extended regions of densely clustered serine (Ser) and/or threonine (Thr) residues bearing O-linked glycans that initiate with α-linked *N*-acetylgalactosamine (GalNAc) (Figure 1A). The closely packed glycans force the polypeptide backbone into an extended structure, giving mucin molecules a rodlike shape.[2] As a consequence, membrane-associated mucins are believed to tower above the surrounding glycocalyx where they are poised to mediate interactions with other biomolecules and cognate cells. Mucins are known to participate in cell adhesion events associated with diseases such as chronic inflammation[3] and cancer metastasis.[4] Secreted mucins, like those forming the major constituents of mucus, have unusual viscoelastic properties and can passivate epithelial cell surfaces.[5] These features have suggested possible roles for mucin-like molecules as biocompatible coatings for synthetic materials.[6]

As a first step in the generation of model cell surfaces, we have focused on the synthesis of mucin-like molecules that can be displayed on model membranes. Small mucin glycopeptide fragments have been generated by several groups using solid-phase peptide synthesis methods.[7] However, the adaptation of such methods to larger, more biologically relevant mucin molecules is not straightforward. To date, the largest full-length mucin glycoprotein constructed using synthetic methods is GlyCAM-1, a rather small polypeptide of 132 residues.[8] The construction of the peptide required a combination of solid-phase glycopeptide synthesis and protein ligation techniques and is not amenable to the generation of analogues tailored for specific applications. Thus, we directed our attention to the

[†] Department of Chemistry, University of California.
[‡] Department of Molecular and Cell Biology, University of California.
[§] Howard Hughes Medical Institute, University of California.
[||] Materials Sciences Division, Lawrence Berkeley National Laboratory.
[⊥] The Molecular Foundry, Lawrence Berkeley National Laboratory.

(1) (a) Hang, H. C.; Bertozzi, C. R. *Bioorg. Med. Chem.* **2005**, *13*, 5021−5034. (b) Fukuda, M. In *Molecular and Cellular Glycobiology;* Fukuda, M., Hindsgaul, O., Eds.; Frontiers in Molecular Biology, Vol. 30, Oxford Univ. Press: New York, NY, 2000; Chapter 1.
(2) Strous, G. J.; Dekker, J. *Crit. Rev. Biochem. Mol. Biol.* **1992**, *27*, 57−92.
(3) Rosen, S. D. *Am. J. Pathol.* **1999**, *155*, 1013−1020.
(4) Hollingsworth, M. A.; Swanson, B. J. *Nat. Rev. Cancer* **2004**, *4*, 45−60.
(5) Gendler, S. J.; Spicer, A. P. *Annu. Rev. Phys.* **1995**, *57*, 607−634.
(6) (a) Coullerez, G.; Seeberber, P. M.; Textor, M. *Macromol. Biosci.* **2006**, *6*, 634−647 and references therein. (b) Holland, N. B.; Qui, Y.; Ruegsegger, M.; Marchant, R. E. *Nature* **1998**, *392*, 799−801.
(7) Pratt, M. R.; Bertozzi, C. R. *Chem. Soc. Rev.* **2005**, *34*, 58−68 and references therein.
(8) Macmillan, D.; Bertozzi, C. R. *Angew. Chem., Int. Ed.* **2004**, *43*, 1355−1359.

10.1021/ja067819i CCC: $37.00 **© 2007 American Chemical Society**

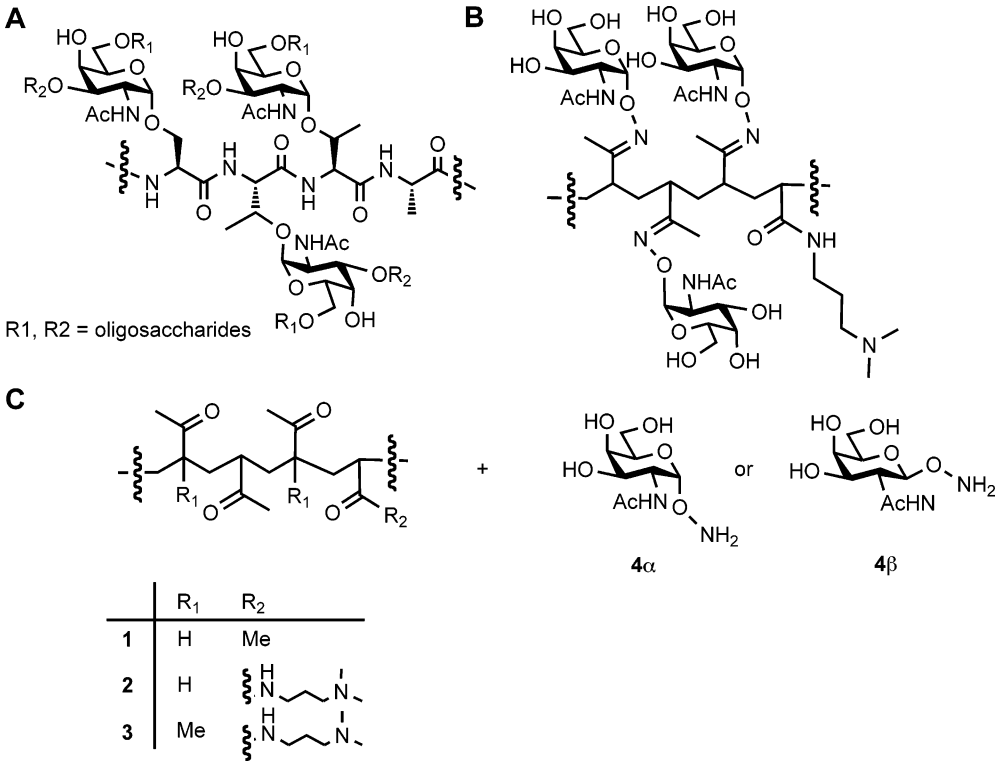

Figure 1. Structures of native mucin segments from (A) the cell-surface protein CD43 and (B) a synthetic mucin mimic. The core GalNAc residue bound to Ser or Thr is often extended with additional sugars at R^1 and R^2. (C) Structures of polymer backbones and glycans employed in this study.

design of mucin mimics that possess the key structural and biological features of native glycoproteins but can be prepared more efficiently.

The dense glycan clusters of mucin glycoproteins are responsible for both their extended rodlike structures and hydrodynamic properties. However, biophysical studies using native mucins have shown that the glycans can be trimmed down to single peptide-bound GalNAc residues without significant loss of structure.[9] 2-D NMR analysis of synthetic mucin fragments containing only six amino acid residues and a cluster of α-linked GalNAc residues revealed a highly structured and extended polypeptide backbone, consistent with a critical role for the core GalNAc residues in governing the overall structure of the mucin biopolymer.[10]

Guided by these observations, we synthesized mucin mimetics comprising a long, synthetically tractable polymer backbone decorated with α-linked GalNAc residues intended to impart backbone rigidity (Figure 1B). The glycan clustering was designed to create unfavorable steric interactions that would be minimized when the polymer chain is fully extended. The oxime linkage by which the sugars are attached to the polymer can be assembled by chemoselective ligation[11] of the corresponding ketone-functionalized polymer (**1**−**3**) with the two anomers of aminooxy GalNAc analog **4α**[12] (Figure 1C). Any aminooxy sugar can be ligated to the polymer backbone in this fashion, including the *β*-anomer of aminooxy GalNAc (**4*β***). This convergent process permits facile modification of either the polymer or sugar components, allowing for the efficient generation of numerous mucin analogues. In this study, we generated mucin mimetics with various polymer backbones derived from methyl vinyl ketone (MVK) (**1** and **2**, Figure 1C) or isopropenyl methyl ketone (IMK) (**3**) combined with the water-solubilizing monomer *N*-[3-(dimethylamino)propyl]-acrylamide (DAPA).[13] Both MVK and IMK introduce ketones into the polymer backbone, but poly(IMK) has additional backbone substitution that we reasoned might contribute to overall rigidity.

With the ultimate goal of constructing model cell surfaces, we further synthesized end-functionalized glycopolymers that insert into lipid bilayers thereby mimicking membrane-bound mucin glycoproteins. These polymers were adorned with various hydrophobic tail groups, including cholesterol, single-chain lipids, and phospholipids.[14] Biophysical characterization of the bilayer-associated mucin mimetics indicated fluid mobility similar to membrane-associated proteins. Finally, we demonstrated that bilayer-associated mucin mimetics can bind specifically to protein receptors. This system provides a novel platform with which to study cell-surface interactions using structurally defined components.

Results and Discussion

Synthesis and Characterization of Mucin Mimetic Polymers. We prepared poly(MVK) (**1**),[13] co-poly(MVK/DAPA) (**2**),[15] and co-poly(IMK/DAPA) (**3**)[16] by radical-induced po-

(9) Shogren, R.; Gerken, T. A.; Jentoft, N. *Biochemistry* **1989**, *28*, 5525−5536.
(10) Live, D. H.; Williams, L. J.; Kuduk, S. D.; Schwarz, J. B.; Glunz, P. E.; Chen, X.-T.; Sames, D.; Kumar, R. A.; Danishefsky, S. J. *Proc. Natl. Acad. Sci. U.S.A.* **1999**, *96*, 3489−3493.
(11) Lemieux, G. A.; Bertozzi, C. R. *Trends Biotechnol.* **1998**, *16*, 506−513.
(12) Marcaurelle, L. A.; Shin, Y.; Goon, S.; Bertozzi, C. R. *Org. Lett.* **2001**, *3*, 3691−3694.
(13) (a) Béraud, V.; Businelli, L.; Gnanou, Y.; Maillard, B.; *Macromol. Rapid Commun.* **2000**, *21*, 901−904. (b) Spaether, W.; Klass, K.; Erker, G.; Zippel, F.; Fröhlich, R. *Chem.—Eur. J.* **1998**, *4*, 1411−1417.
(14) Nosjean, O.; Briolay, A.; Roux, B. *Biochim. Biophys. Acta* **1997**, *1331*, 153−186.
(15) (a) Zhong, X.-D.; Ishifune, M.; Nakao, N.; Yamashita, N. *J. Macromol. Sci.-Chem. Pure and Appl. Chem.* **1999**, *A36*, 287−303. (b) Tsuneka, T.; Ishifune, M.; Yamashita, N. *J. Macromol. Sci., Pure Appl. Chem.* **1994**, *A31*, 1169−1176. (c) Yamashita, N.; Ikezawa, K.; Ayukawa, S.-I.;

Scheme 1. Synthesis of Polymers Functionalized with GalNAc Residues[a]

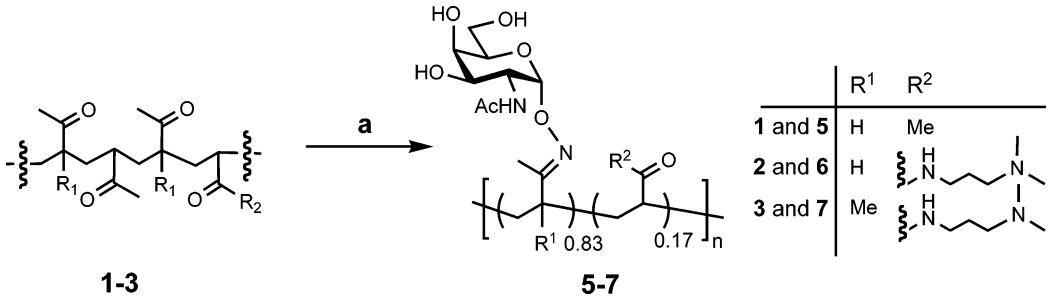

[a] Conditions: (a) **4α** (2.8 equiv), CH_3Cl/H_2O, AcOH, 95 °C.

Table 1. Apparent Molecular Weights (M_w) and Hydrodynamic Diameters (D_h) of the GalNAc-Ligated and Unligated Polymers

	unligated M_w (g/mol)[a]	ligated M_w (g/mol)[b]	unligated D_h (nm)	ligated D_h (nm)[d]	calcd length[e]	% extension
5	18330	72530	1.9[c]	54.0	66.8	81
6	32500	102880	2.0[c]	54.7	95.8	57
7	29690	72530	2.1[d]	65.0	78.5	83

[a] Molecular weights were determined by GPC based on a polystyrene standard curve. [b] Molecular weights were determined by GPC based on a polysaccharide standard curve. [c] Hydrodynamic radii were measured in THF. [d] Hydrodynamic radii were measured in water. [e] Values were calculated for the fully extended polymers based on their apparent molecular weights, using MM2 force field-based molecular mechanics predictions.

lymerization using literature procedures. Copolymers **2** and **3** were generated using 4.4 equiv of MVK or 5.0 equiv of IMK, resulting in copolymers with similar monomer ratios (Scheme 1, ~4.7 MVK or IMK/DAPA based on elemental analysis). α-Aminooxy GalNAc (**4α**) was prepared using our previously reported procedure.[12] The polymers were combined with compound **4α** (2−3 equiv per ketone) in water with 0.1% AcOH for 96 h at 95 °C, then dialyzed to remove unreacted sugar. In the case of poly(MVK), acetonitrile (75%) was used as a cosolvent. The GalNAc-conjugated polymers **5**, **6**, and **7** (Scheme 1) were lyophilized and characterized by IR and NMR spectroscopy, gel permeation chromatography (GPC), and elemental analysis.

To determine the extent of ketone ligation, we measured the change in apparent molecular weight (M_w) of the polymers after reaction with compound **4α** using GPC. The M_w ratio of GalNAc-conjugated **5** to unmodified poly(MVK) (**1**) was found to be 3.96 (Table 1). The theoretical M_w ratio corresponding to 100% ketone conjugation was calculated to be 4.11. Thus, the chemoselective ligation reaction was nearly quantitative. Analysis of polymers **6** and **7** yielded similar results.

To determine the consequences of sugar clustering on the overall structures of the polymers, we compared the effective hydrodynamic diameters (D_h) of the GalNAc-conjugated and unmodified polymers using dynamic light scattering. The light scattering behavior of each polymer was fitted to that of an equivalent sphere. No corrections for nonspherical shape were made as the expected difference between extended and globular polymers is large.[9] The measured D_h values for the unmodified polymers **1**, **2**, and **3** were 1.9, 2.0, and 2.1 nm, respectively. Given the apparent molecular weights of 18330, 32500, and 29690, respectively, derived from GPC data (Table 1), these D_h values indicate a globular structure. (D_h was measured in THF for **1**, and in water for **2** and **3**; solubility limitations prevented D_h measurements for **1** in water.) The D_h values of the GalNAc-conjugated polymers **5**, **6**, and **7** were 54.0, 54.7, and 65.0 nm, respectively, implying a more extended structure. The theoretical fully extended lengths of **5**, **6**, and **7** were calculated[17] to be 66.8, 95.8, and 78.5 nm, respectively (Table 1). By comparing these values to the measured D_h values for the GalNAc-conjugated polymers, we estimated the percent extension of the polymer backbones to be 81% for **5**, 57% for **6**, and 83% for **7**. Thus, the rigidification imposed by glycosylation was more significant for polymers **5** and **7** than for polymer **6**. Polymer **5** lacks DAPA monomers and therefore possesses a higher density of GalNAc residues, while methylation of the backbone in **7** might add steric bulk and restrict conformational freedom. In all three cases, GalNAc clustering on the polymer backbone led to a more extended conformation, similar to what is observed with native mucins.

The configuration of the mucin mimetics was further assessed by transmission electron microscopy (TEM) analysis of polymer **5** (Figure 2). Individual polymer molecules could be seen as rods with lengths of 20−80 nm, consistent with the light scattering data. Thus, on the basis of both light scattering and TEM data, we conclude that the GalNAc-conjugated polymers adopt an extended configuration while the parent, nonglycosylated polymers, do not.

Modular Synthesis of End-Functionalized Mucin-Mimetic Polymers. The application of these mucin-mimetic polymers as model systems for cell-surface studies or as coatings for biomaterials required their end functionalization with moieties that can associate with hydrophobic or amphiphilic surfaces. Toward this end, we first generated two lipid-modified AIBN derivatives, **8** and **9** (Figure 3), for use as radical initiators.[18] The compounds were prepared by EDC-mediated coupling of octadecylamine or cholesterol, respectively, with 4,4′-azobis-(4-cyanovaleric acid) (ACVA). Heating the free radical initiators in the presence of MVK at 95 °C for 72 h afforded the end-functionalized keto-polymers **10** and **11** (Scheme 2). Compound **4α** was coupled to the keto-polymers to generate oxime-linked glycopolymers **12** and **13**, bearing octadecyl and cholesteryl

Maeshima, T. *J. Macromol. Sci., Pure Appl. Chem.* **1984**, *A21*, 615−629.
(16) (a) Merle-Aubry, L.; Merle, Y. *Eur. Polymer J.* **1980**, *16*, 227−234. (b) Greenley, R. Z. *J. Macromol. Sci., Pure Appl. Chem.* **1980**, *A14*, 427−443. (c) Greenley, R. Z. *J. Macromol. Sci., Pure Appl. Chem.* **1980**, *A14*, 445−515. (d) Lyons, A. R.; Catterall, E. *Eur. Polymer. J.* **1971**, *7*, 839. (e) Lyons, A. R.; Catterall, E. *Eur. Polymer. J.* **1971**, *7*, 849−862.
(17) Molecular models were constructed using the MM2 energy minimization algorithm in CS Chem 3D Pro (version 5.0).
(18) (a) Winnik, F. M.; Davidson, A. R.; Hamer, G. K. *Macromolecules* **1992**, *25*, 1876−1880. (b) Sugiyama, K.; Shiraishi, K.; Matsumoto, T. *J. Polym. Sci., Part A: Polym. Chem.* **2003**, *41*, 1992−2000.

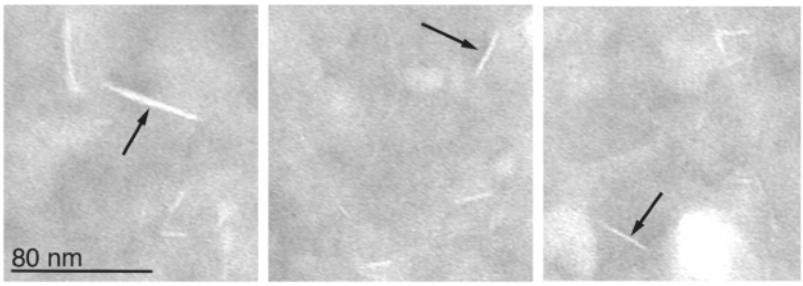

Figure 2. Transmission electron micrographs of polymer **5** negatively stained with 1% phosphotungstic acid (PTA). The three panels are representative fields from the same carbon grid. Arrows indicate individual polymer molecules.

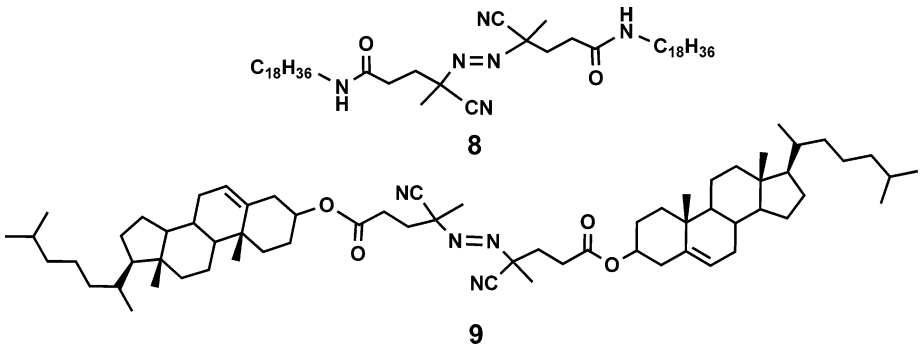

Figure 3. End-functionalized free radical initiators.

Scheme 2. Synthesis of End Functionalized Polymers[a]

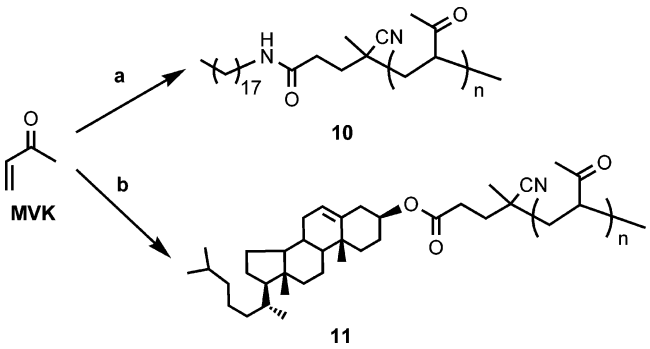

[a] Conditions: (a) **8**, *p*-dioxane, 95 °C, 72 h; (b) **9**, toluene, 95 °C, 72 h.

groups, respectively (Scheme 3). For biophysical studies, we also generated an octadecyl-functionalized glycopolymer bearing a small percentage of the fluorescent dye Texas Red. This was accomplished by coupling keto-polymer **10** with a mixture of compound **4α** (2.8 equiv) and Texas Red hydrazide (0.03 equiv), affording fluorescent mucin mimetic **14** (Scheme 3).

In preliminary experiments, we attempted to integrate lipid-terminated mucin mimetic **14** into synthetic lipid bilayers that were generated using previously described techniques.[19] Briefly, two-dimensionally fluid, solid-supported membranes were formed on SiO_2 substrates by standard vesicle-fusion techniques. Polymer **14** was incubated with the lipid membranes at a concentration of 20 μg/mL for 15 h. However, fluorescence microscopy analysis indicated that only a small amount of polymer incorporated into the membrane, which was insufficient for subsequent studies. Similar results were obtained with the analogous cholesteryl-functionalized polymer. Nonetheless, octadecyl-terminated mucin mimetics **13** and **14** proved useful as coatings for carbon nanotubes[20] and have since been used to interface the nanotubes with live cells.[21]

To enhance the incorporation of mucin mimetics into supported bilayers, we sought to increase the lipophilicity of the end groups. Accordingly, we designed a second-generation end-functionalized polymer with a phospholipid tail that is more similar to biological membrane components. EDC-mediated coupling of ACVA with dipalmitoylphosphatidylethanolamine (DPPE) was unsuccessful. Thus, we converted ACVA to the bispentafluorophenyl (PFP) ester **15**, which was directly coupled with DPPE. The bis-DPPE AIBN analogue **16** could not be isolated and was carried on directly to the polymerization reaction. Heating compound **16** in the presence of MVK at 95 °C for 72 h afforded the end-functionalized polymer **17** (Scheme 4). As accomplished previously, compound **4α** was coupled to the polymer along with a small amount of Texas Red hydrazide to afford polymer **18**. In parallel, we generated a similar polymer adorned with the β-anomer of GalNAc **(19)** by coupling compound **4*β*** (Figure 1C) with keto-polymer **17** (Scheme 5).

Glycan elaboration of the keto-polymer backbone is not limited to simple monosaccharides. Taking advantage of the modular polymer design, we elaborated the end-functionalized polymer **17** with β-aminooxy-*N*-acetyl lactosamine (β-aminooxy LacNAc).[22] Using the conditions established for **4α** and **4*β***, β-aminooxy LacNAc was coupled to **17** with a small amount of Texas Red hydrazide to afford polymer **20** (Scheme 5).

Incorporation of Mucin Mimetics into Fluid Lipid Bilayers. Phospholipid-functionalized polymers **18** and **19**, which differ only in the anomeric linkage of the pendent GalNAc residues, and polymer **20**, containing LacNAc residues, were incubated with supported bilayers for 15 h at a concentration

(19) (a) Boxer, S. G. *Curr. Opin. Chem. Biol.* **2000**, *4*, 704−709. (b) Richter, R. P.; Berat, R.; Brisson, A. R. *Langmuir* **2006**, *22*, 3497−505.

(20) Chen, X.; Lee, G. S.; Zettl, A.; Bertozzi, C. R. *Angew. Chem., Int. Ed.* **2004**, *43*, 6111−6116.

(21) Chen, X.; Tam, U. C.; Czlapinski, J. L.; Lee, G. S.; Rabuka, D.; Zettl, A.; Bertozzi, C. R. *J. Am. Chem. Soc.* **2006**, *128*, 6292−6293.

(22) Rodriguez, E. C.; Marcaurelle, L. A.; Bertozzi, C. R. *J. Org. Chem.* **1998**, *63*, 7134−7135.

Scheme 3. Ligation of GalNAc Derivatives to the Polyketone Polymer Backbone[a]

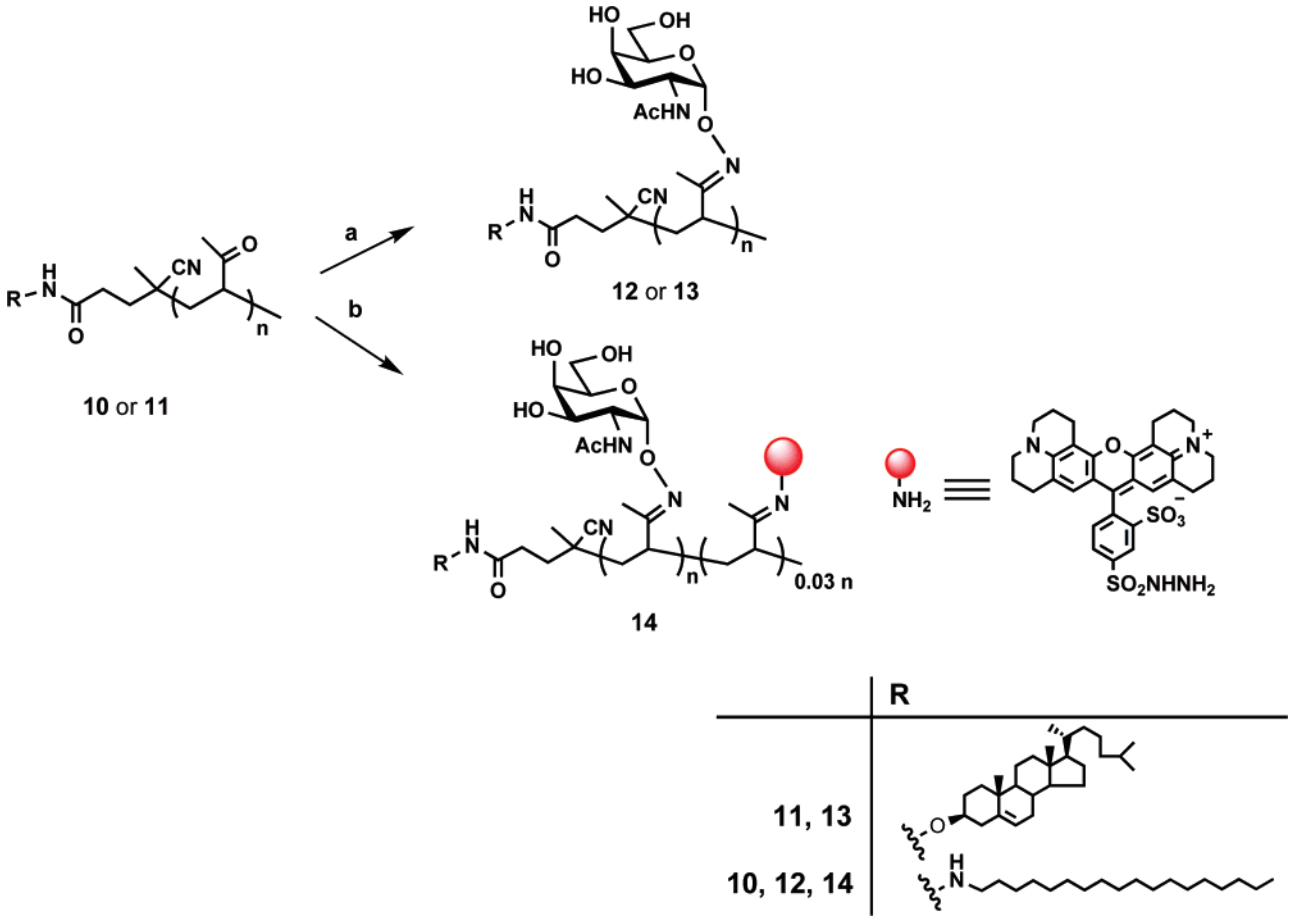

[a] Conditions: (a) **4α** (2.8 equiv), CH_3CN/H_2O (3:1), AcOH, 95 °C; (b) **4α** (2.8 equiv), Texas Red hydrazide (0.03 equiv), CH_3CN/H_2O (3:1), AcOH, 95 °C.

of 20 μg/mL, and the unbound polymer was removed by washing (shown schematically in Figure 4A). Fluorescence analysis indicated robust association with the supported bilayers, in stark contrast to the single lipid chain analogue **14** discussed above. Fluorescence quantitation of the Texas Red-labeled glycopolymers gave an estimated density of around 500 molecules/μm^2 in the supported bilayer. In a control experiment, we bound polymer **18** directly to a glass substrate lacking a supported bilayer. In this case, the observed polymer density was only 20 molecules/μm^2, barely above the detection limit of our fluorescence microscope, indicating that adsorption to the underlying substrate is minimal.

Lateral mobility is a characteristic feature of biological membrane-associated proteins that permits the dynamic formation of functional complexes and aggregates. To address the biological relevance of our synthetic model system, we investigated the mobility of the membrane-bound mucin mimetics using the fluorescence recovery after photobleaching (FRAP) technique.[23] Supported bilayers incorporating polymer **18** were irradiated with 560 nm light for 10 s and were monitored over several minutes (Figure 4B). This experiment yielded a diffusion coefficient for the mucin mimetic **18** of 2.7 ± 1.5 μm^2/s. Polymers **19** and **20** behaved similarly to **18** in all regards.

In parallel, we determined the intrinsic lipid mobility of the membranes by measuring the diffusion coefficient of Texas Red-modified 1,2-dihexadecanoyl-*sn*-glycero-3-phosphoethanolamine using the FRAP method. The measured value of 2.3 ± 0.8 μm^2/s was similar to that of the mucin mimetic, suggesting that polymer **18** was anchored to the membrane solely by its lipid moiety and not via strong lipid−sugar interactions. To our knowledge, this is the first report of mobile glycosylated polymers anchored to a supported lipid bilayer.

Interaction of Membrane-Associated Mucin Mimetics with Proteins. A major function of cell-surface mucins is to guide interactions among cells via specific molecular recognition by carbohydrate-binding proteins. We therefore assessed the ability of mucin mimetics **18** and **19** to bind carbohydrate-binding proteins (i.e., lectins) while presented on supported bilayers. *Helix pomatia* agglutinin (HPA) is known to specifically bind α-linked GalNAc residues but does not interact significantly with the β-anomer.[24] Conversely, *Bauhinia purpurea* agglutinin (BPA) binds to β-linked GalNAc residues, but not to the α-anomer.[25] Both lectins are available in fluorescein isothiocyante (FITC)-labeled form.

Supported lipid bilayers containing Texas Red-labeled mucin mimetics **18** or **19** (∼500 molecules/μm^2), or no polymer, were incubated with FITC-labeled lectin (30 μg/mL, 60 min), which had been filtered prior to incubation, and then washed to remove unbound protein. The membrane-associated fluorescence derived from FITC or Texas Red was quantified by microscopy, and

(23) Axelrod, D.; Koppel, D. E.; Schlessinger, J.; Elson, E.; Webb, W. W. *Biophys. J.* **1976**, *16*, 1055−1069.
(24) Sharon, N. *Adv. Immunol.* **1983**, *34*, 213−298.
(25) Sharon, N.; Lis, H. *J. Agric. Food Chem.* **2002**, *50*, 6586−6591.

Scheme 4. Synthesis of Phosphobilipid End Functionalized AIBN[a]

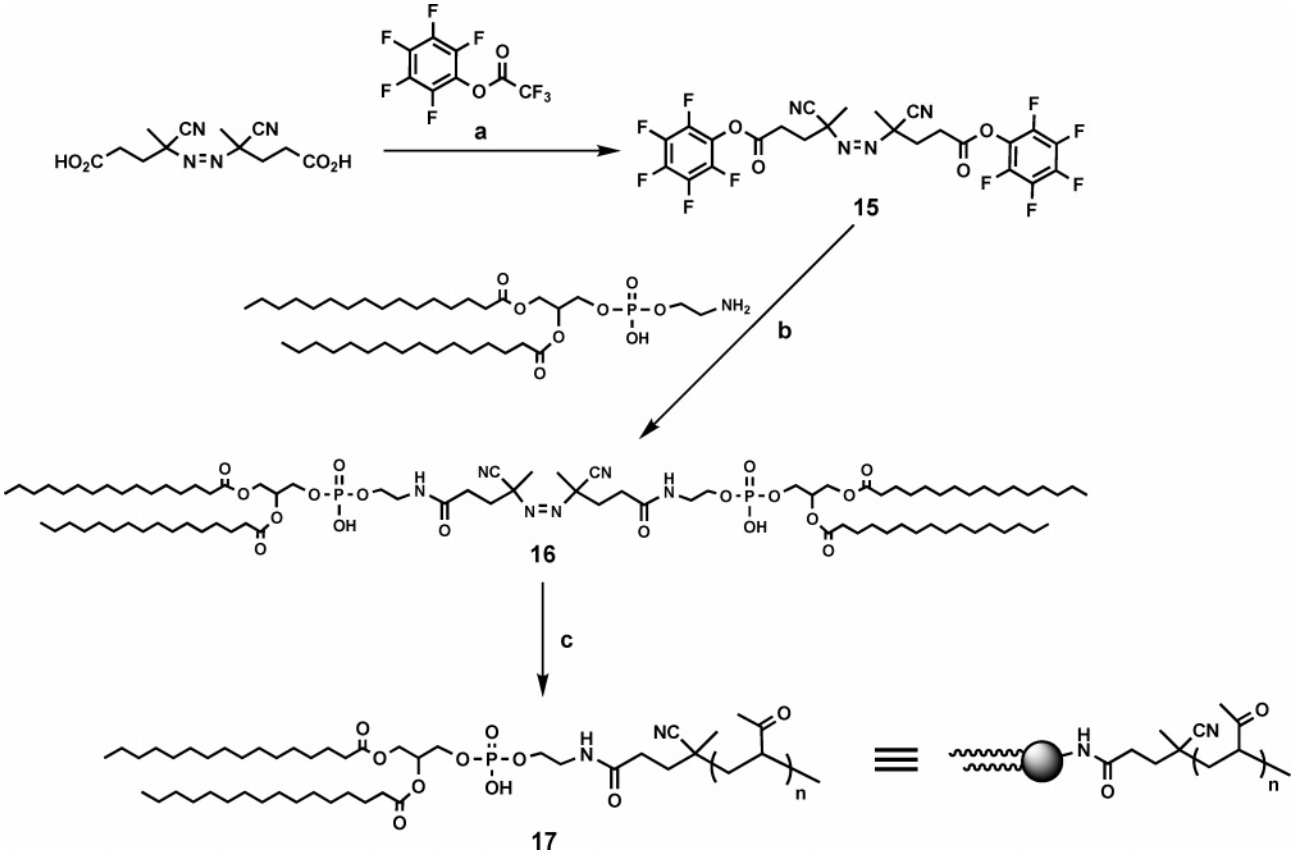

[a] Conditions: (a) DIPEA, CH_3CN, 43%; (b) $CHCl_3$/MeOH (3:1); (c) MVK, toluene, 95 °C, 24 h.

the ratios of these fluorescence intensities were compared for each lectin (Figure 5A). The amount of HPA bound to membranes bearing polymer **18** (α-GalNAc/MVK) was significantly higher (8-fold) than that bound to membranes with polymer **19** (*β*-GalNAc/MVK). Conversely, the amount of BPA bound to membranes presenting polymer **19** exceeded that bound to membranes displaying polymer **18** by 36-fold. Bilayers with no associated mucin mimetics showed no detectable lectin binding (not shown). Thus, the specificities of the lectins as determined in biological systems are accurately recapitulated in this biomimetic system.

Supported lipid bilayers containing Texas Red-labeled polymer **20** were also probed for lectin binding activity using FITC-conjugated *Erythrina cristagalli* agglutinin (ECA), which is known to bind the LacNAc motif.[26] As shown in Figure 5B, FITC-ECA labeled these bilayers with a 30-fold stronger signal than observed with FITC-HPA.

Conclusions

In summary, the mucin mimetic polymers described here possess structural features similar to natural mucins but are far more synthetically tractable. With appropriate lipid end-functionalization, the polymers can be incorporated into fluid lipid bilayers where they demonstrate mobility similar to natural membrane-associated biomolecules. Finally, the mucin mimetics interact with carbohydrate-binding proteins in a specific fashion.

The repertoire of cell-surface glycans is known to change during cell differentiation and malignant transformation.[27] Notably, the sugar substituents on our mucin mimetics can be readily altered by chemical methods or elaborated enzymatically to provide a range of glycan structures that reflect various cell states. Thus, the system may be amenable to fundamental studies of cell-surface interactions relevant to stem cell differentiation or metastasis.

Although prevalent on cell surfaces, mucins are only one component of a diverse landscape that includes thousands of additional protein and lipid molecules. Thus, the model cell surfaces generated in this study represent early intermediates in the bottom-up assembly of multifunctional surfaces that act as a complex system. Integration of additional biomolecules into this system is a current goal.

Experimental Methods

General Methods. All chemical reagents were of analytical grade, obtained from commercial suppliers, and used without further purification unless otherwise noted. 1,2-Dioleoyl-*glycero*-3-phosphocholine (DOPC) and 1,2-dioleoyl-3-trimethylammonium-propane (DOTAP) were purchased from Avanti Polar Lipids. 1,2-Dihexadecanoyl-glycero-3-phosphoethanolamine conjugated to the fluorophore Texas Red (Texas Red DHPE) was purchased from Invitrogen. The fluorescein-conjugated lectins *Helix pomatia* agglutinin (HPA), *Bauhinia purpurea* agglutinin (BPA), and *Erythrina cristagalli* agglutinin (ECA) were purchased from EY Laboratories (San Mateo, CA). Flash chromatography was performed using Merck 60 Å 230−400 mesh silica gel. Analytical thin layer chromatography (TLC) was performed on glass-backed Analtech Uniplate silica gel plates, and compounds were visualized by staining

(26) De Boeck, H.; Loontiens, F. G.; Lis, H.; Sharon, N. *Arch. Biochem. Biophys.* **1984**, *234*, 297−304.

(27) Fuster, M. M.; Esko, J. D. *Nat. Rev. Cancer* **2005**, *5*, 526−42.

Scheme 5. Ligation of GalNAc Derivatives and Texas Red Hydrazide to the Polymer Backbone[a]

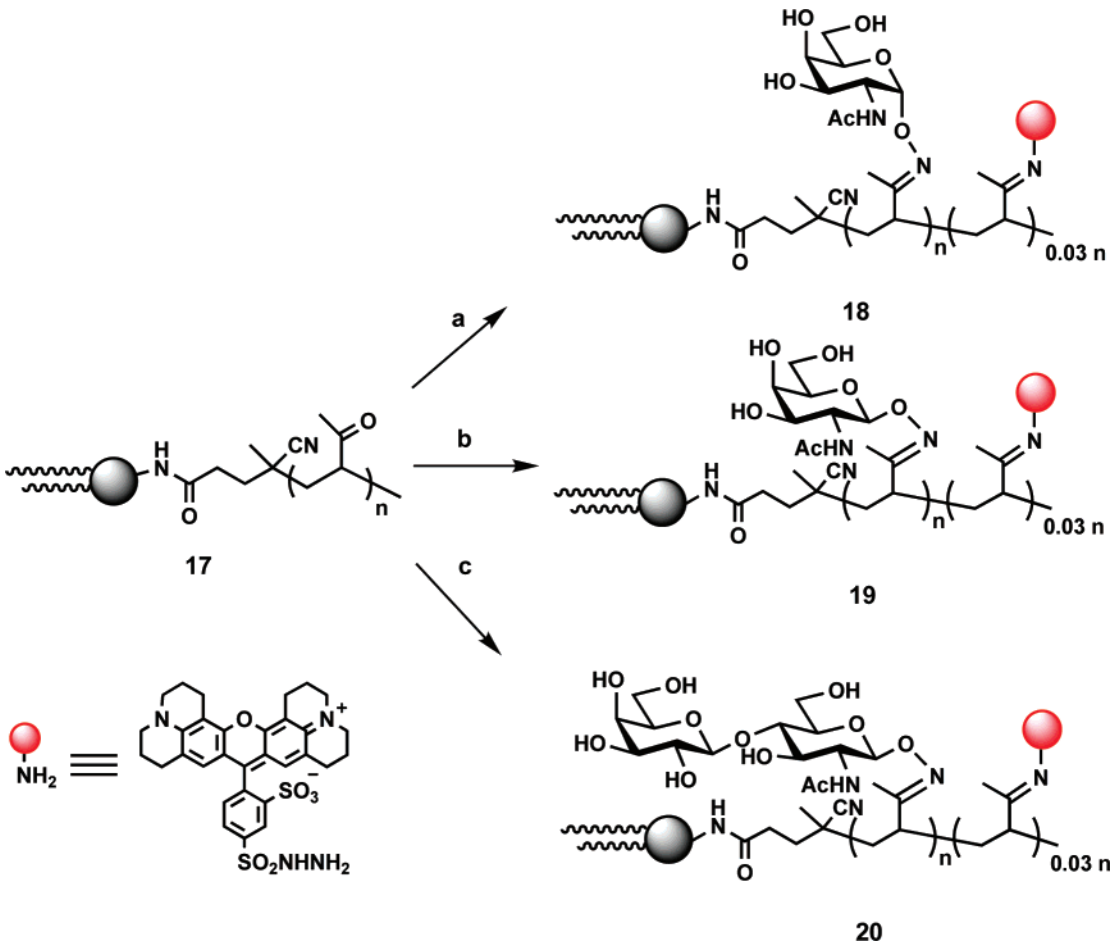

[a] Conditions: (a) **4*β***, Texas Red hydrazide, CH_3CN/H_2O, AcOH, 95 °C; (b) **4*β***, Texas Red hydrazide, CH_3CH/H_2O, AcOH, 95 °C; (c) *β*-aminooxy LacNAc, Texas Red hydrazide, CH_3CN/H_2O, AcOH, 95 °C.

with phosphomolybdic acid, 10% H_2SO_4 in ethanol, and/or the absorbance of UV light. All reaction solvents were distilled under a nitrogen atmosphere prior to use. CH_2Cl_2, pyridine, and toluene were dried over CaH_2. Unless otherwise specified, all solvents were removed under reduced pressure using a rotary evaporator. ^1H NMR and ^{13}C NMR spectra were obtained at 400 and 100 MHz, respectively, using a Bruker AVQ-400 spectrometer. Chemical shifts are reported in parts per million (ppm) relative to tetramethylsilane, and coupling constants (*J*) are reported in hertz (Hz). Infrared (IR) spectra were obtained using a Perkin-Elmer 1600 series Fourier transform infrared spectrometer (FTIR). Low and high-resolution fast atom bombardment (FAB) mass spectra were obtained at the UC Berkeley Mass Spectrometry Laboratory. Electrospray ionization (ESI) mass spectra were obtained with a Hewlett-Packard series 1100 mass spectrometer. Gel permeation chromatography (GPC) with THF as an eluent was carried out using a system composed of a Waters 510 pump with a Waters 717 auto sampler, 500 Å PLgel columns thermostated at 35 °C, and an Optilab DSP differential refractometer thermostated at 35 °C. The GPC data were analyzed using Empower software (Waters) based on polystyrene and polysaccharide standards to calculate the polydispersity (PDI). TEM images were obtained on a FEI Tecnai 12 120 KV microscope operating at electron energy of 100 keV. Samples were prepared by depositing an aqueous solution (0.05 mg/mL) onto carbon-coated copper grids. The solution was allowed to absorb on the grids for 2 min followed by staining the material with 1.0% phosphotungstic acid.

Conjugation of Aminooxy 2-Acetamido-2-deoxy-α-D-galactopyranoside (4α) to Poly(MVK) (1) To Form GalNAc-Conjugated Polymer (5). Acetonitrile (6 mL) was introduced into a 25-mL flask containing poly(MVK) (**1**) (11.6 mg, 0.165 mmol based on carbonyl number) and **4α**[12] (77.9 mg, 0.330 mmol). Aqueous acetic acid (0.5%, 2 mL) was added to the mixture in order to dissolve compound **4α**. After heating at reflux for 24 h, the reaction mixture was allowed to cool to room temp. All solvents were removed in vacuo, and then deionized water (2 mL) was introduced into the mixture to dissolve the partially ligated water-soluble polymer. After heating at reflux for 24 h to effect full ligation, the reaction mixture was cooled to room temp, dialyzed against water to remove excess compound **4α**, neutralized with Dowex 50WX8-100 resin, and lyophilized to afford **5** as a fluffy white solid. ^1H NMR (D_2O, δ/ppm, see Figure SI-1b); IR (KBr, cm^{-1}) 3396, 2932, 1653, 1542, 1374, 1116, 1054, 915 (see Figure SI-2b); Hydrodynamic radius (27.0 nm in water, 0.3 mg/mL, see Figure SI-3b). $M_w = 72530$. Anal. Calcd for $(C_{12}H_{20}N_2O_6)_n$: C, 49.99; H, 6.99; N, 9.72. Found: C, 48.36; H, 6.96; N, 9.82.

Conjugation of (4α) to Co-poly(MVK/DAPA) (2) To Form GalNAc-Conjugated Polymer (6). A solution of 0.1% aqueous acetic acid (2 mL) was introduced into a 25-mL flask containing co-poly-(MVK/DAPA) (**2**) (18.6 mg, 0.174 mmol based on carbonyl number) and compound **4α** (80.1 mg, 0.339 mmol). After 4 d at 95 °C, the reaction mixture was cooled to room temp, dialyzed in water to remove excess compound **4α**, neutralized with Dowex 50WX8-100 resin, and lyophilized to afford **6** as a fluffy white solid. ^1H NMR (D_2O, δ/ppm, see Figure SI-4b); IR (KBr, cm^{-1}) 3398, 2932, 1655, 1542, 1375, 1119, 1054 (see Figure SI-5b); Hydrodynamic radius (27.4 nm in water, 0.3 mg/mL, see Figure SI-6b). $M_w = 102880$. Anal. Calcd for $(C_{11.24}H_{19.24}N_{2.00}O_{5.05})_n$: C, 51.29; H, 7.37; N, 10.64. Found: C, 50.77; H, 7.36; N, 10.82.

Conjugation of (4α) to Co-poly(IMK/DAPA) (3) To Form GalNAc-Conjugated Polymer (7). A solution of 0.1% aqueous acetic

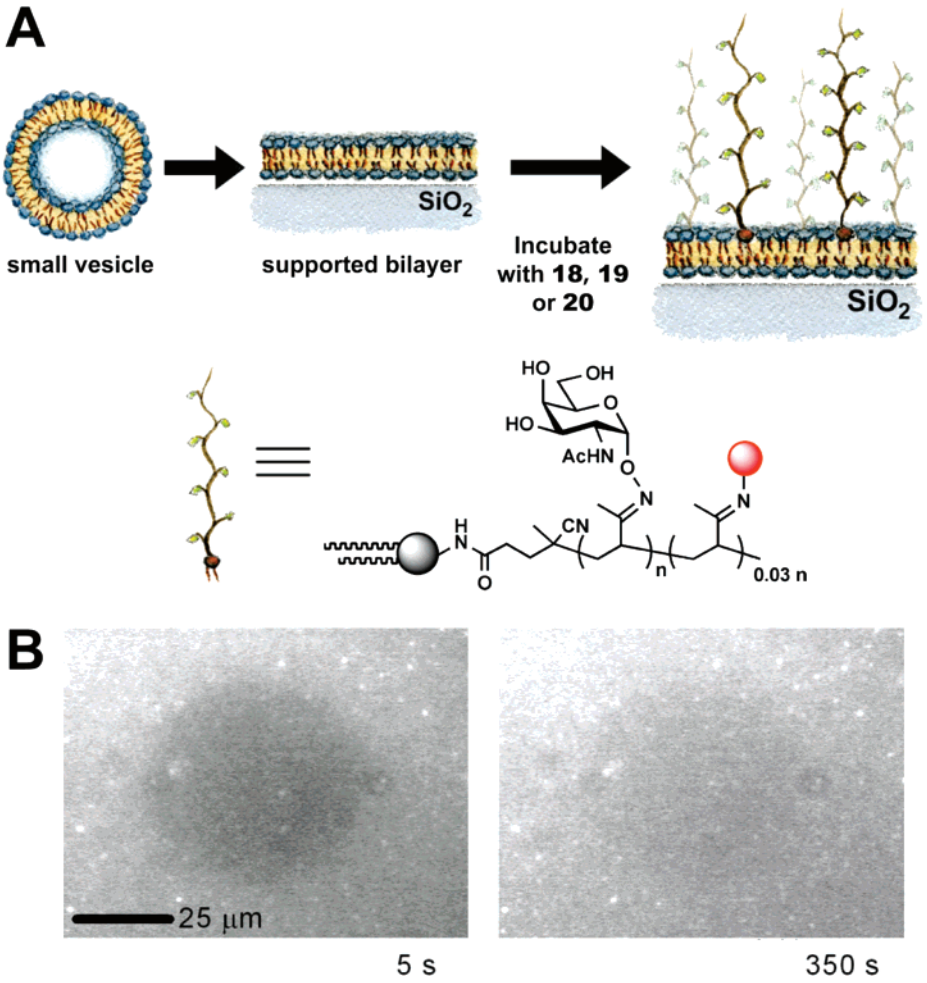

Figure 4. (A) Schematic of supported lipid bilayer formation from small liposomes, and polymer incorporation in a supported lipid bilayers; (B) fluorescence images of **18** incorporated into a supported lipid bilayer. Fluorescence recovery after photobleaching (FRAP) demonstrates the fluidity of the membrane-anchored mucin mimics. (left) Fluorophores conjugated to the polymer were bleached in the central zone; (right) after 350 s. Bleached and unbleached molecules have diffused, leading to recovery of the dark zone's fluorescence. Analysis revealed a diffusion coefficient identical to that of the membrane lipids.

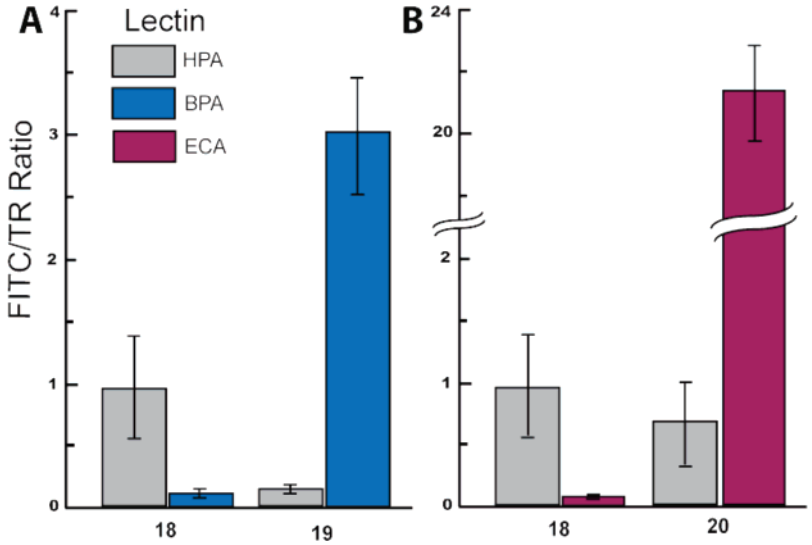

Figure 5. (A) Lectin binding to **18** or **19** displayed on supported bilayers. HPA exhibits a stronger binding to **18** (α-GalNAc) while BPA exhibits a stronger affinity for **19** (*β*-GalNAc). (B) Lectin binding to **18** or **20** displayed on supported bilayers. ECA exhibits a stronger affinity for **20** (*β*-LacNAc). The carbohydrate specificities of the lectin bindings replicate those seen in natural biological systems. Error bars indicate the standard deviation for 3 replicate experiments.

acid (2 mL) was introduced into a 25-mL flask containing co-poly-(IMK/DAPA) (**3**) (19.1 mg, 0.165 mmol based on carbonyl number) and compound **4α** (110 mg, 0.466 mmol). After 7 d at 95 °C, the reaction mixture was allowed to cool to room temp, dialyzed in water

to remove excess compound **4α**, neutralized with Dowex 50WX8-100 resin, and lyophilized to afford **7** as a fluffy white solid. ^{1}H NMR (D_2O, δ/ppm, see Figure SI-7b); IR (KBr, cm^{-1}) 3436, 2956, 2925, 1653, 1559, 1458, 1375, 1117(see Figure SI-8b); Hydrodynamic radius (32.5 nm in water, 0.3 mg/mL, see Figure SI-9b). M_w = 85630. Anal. Calcd for $(C_{12.15}H_{20.98}N_{2.00}O_{5.15})_n$: C, 52.59; H, 7.62; N, 10.10. Found: C, 51.27; H, 7.53; N, 10.28.

C18-Azobis(4-cyanovaleric acid) (8). To a solution of 4,4′-azobis-(4-cyanovaleric acid) (590 mg, 2.11 mmol) in CH_2Cl_2 (100 mL) was added 4-(dimethylamino)pyridine (260 mg, 2.11 mmol), triethylamine (1.20 mL, 8.61 mmol), and octadecylamine (2.27 g, 8.44 mmol). The solution was stirred for 15 min and *N*-(3-dimethylaminopropyl)-*N*′-ethylcarbodiimide hydrochloride (1.62 g, 8.44 mmol) was added. The solution was stirred in the dark for 18 h under N_2, diluted with CH_2Cl_2, and washed with brine (250 mL) and water (250 mL). The organic layer was dried over Na_2SO_4, filtered, and concentrated in vacuo. The resulting solid was purified on a silica gel column (hexanes/ethyl acetate, 2:1) to afford compound **8** (980 mg, 59%) as a white solid: mp 102−104 °C. IR (thin film): 2916, 2848, 2026, 1614, 1520, 1398, 776 cm^{-1}. ^{1}H NMR (400 MHz, $CDCl_3$): δ 0.80 (t, 6 H, J = 6.3), 1.49 (t, 6 H, J = 6.8), 1.67−1.76 (m, 31 H), 1.78−1.81 (m, 6 H), 2.13−2.23 (m, 6 H), 2.40−2.49 (m, 18 H), 3.20−3.27 (m, 12 H), 5.74−5.77 (m, 4 H), 5.93−5.95 (m, 2 H). ^{13}C NMR (100 MHz, $CDCl_3$): δ 14.09, 22.66, 26.91, 29.33, 29.45, 29.55, 29.67, 31.89, 39.80, 72.56, 171.64. HRMS-(FAB): Calcd for $C_{48}H_{91}LiN_6O_2$ $[M+Li]^+$, 783.7203; found, 783.7197. Anal. Calcd for $C_{49}H_{93}N_6O_3 \cdot H_2O$: C, 73.54; H 11.71; N, 8.75. Found: C, 73.72; H, 11.97; N, 8.66.

C18-Poly(MVK) (10). Anhydrous *p*-dioxane (0.56 mL) was introduced into a 10 mL Schlenk tube containing methyl vinyl ketone (0.56 mL, 6.73 mmol) and **8** (50 mg, 0.064 mmol) under N_2. The reaction mixture was stirred for 72 h at 95 °C after degassing by four freeze−pump−thaw cycles. The reaction mixture was allowed to cool to room temp, diluted with *p*-dioxane (5 mL), and added dropwise to excess diethyl ether (1 L) with vigorous stirring. The precipitate was filtered, washed with diethyl ether, and dried in vacuo overnight to afford **10** as a white solid (325 mg). IR (thin film): 2926, 1709, 1426, 1356, 1239, 1163, 1109, 734 cm^{-1}. ^{1}H NMR (400 MHz, $CDCl_3$, δ/ppm, see Figure SI-11); GPC (THF eluent, polystyrene standard), M_w = 2.18 × 10^5 Da, PDI = 2.20. Anal. Calcd for $(C_4H_6O)_n$: C, 68.54; H, 8.63. Found: C, 67.98; H, 8.93.

Cholesterol-poly(MVK) (11). Anhydrous toluene (0.56 mL) was introduced into a 10 mL Schlenk tube containing methyl vinyl ketone (0.56 mL, 6.7 mmol) and **9** (50 mg, 0.064 mmol) under N_2. The reaction mixture was stirred for 72 h at 95 °C after degassing by four freeze−pump−thaw cycles. The reaction mixture was allowed to cool to room temp, diluted with toluene (5 mL), and then added dropwise to excess diethyl ether (1 L) with vigorous stirring. The precipitate was filtered and washed with diethyl ether then dried overnight in vacuo to afford **11** as a white solid (450 mg). IR (thin film): 3400, 2932, 1708, 1425, 1356, 1240, 1163, 958, 734 cm^{-1}. ^{1}H NMR (400 MHz, $CDCl_3$, δ/ppm, see Figure SI-12); GPC (THF eluent, polystyrene standard), M_w = 1.71 × 10^5 Da, PDI = 1.77. Anal. Calcd for $(C_4H_6O)_n$: C, 68.54; H, 8.63. Found: C, 69.98; H, 7.91.

α-Aminooxy GalNAc C18-Poly(MVK) (12). To a solution of **10** (3.0 mg, 0.043 mmol based on carbonyl number) in THF (3 mL) and H_2O (1 mL) was added **4α** (28 mg, 0.120 mmol) and acetic acid (5 μL). The reaction mixture was stirred at 95 °C for 24 h, allowed to cool to room temp and concentrated in vacuo. The resulting solid was dissolved in H_2O (4 mL) and heated to reflux for 48 h. The reaction mixture was cooled to room temp, dialyzed in H_2O, and lyophilized to give **12** (12 mg, 87% carbonyls reacted) as a fluffy white solid. IR (KBr): 3435, 1641, 1384, 1013, 664, 576 cm^{-1}. ^{1}H NMR (400 MHz, D_2O, δ/ppm, see Figure SI-13); GPC (H_2O eluent, polysaccharide standard), M_w = 30.0 × 10^3 Da, PDI = 2.80. Anal. Calcd for $(C_{12}H_{20}N_2O)_n$: C, 49.99; H, 6.99; N, 9.82. Found: C, 47.04; H, 7.71; N, 7.82.

α-Aminooxy GalNAc Cholesterol-poly(MVK) (13). To a solution of **11** (3.0 mg, 0.043 mmol based on carbonyl number) in THF (3 mL) and H_2O (1 mL) was added **4α** (28 mg, 0.12 mmol) and acetic acid (5 μL). The solution was heated to 95 °C, stirred for 24 h and concentrated in vacuo. The resulting solid was dissolved in H_2O (4 mL) and heated at reflux for 48 h. The reaction mixture was cooled to room temp, dialyzed in H_2O, and lyophilized to give **13** (11 mg, 80% of carbonyls reacted) as a fluffy white solid. IR (KBr): 3483, 1658, 1641, 1005, 565 cm^{-1}. ^{1}H NMR (400 MHz, D_2O, δ/ppm, see Figure SI-14); GPC (H_2O eluent, polysaccharide standard), M_w = 30.9 × 10^3 Da, PDI = 3.18. Anal. Calcd for $(C_{12}H_{20}N_2O)_n$: C, 49.99; H, 6.99; N, 9.82. Found: C, 50.79; H, 7.98; N, 6.56.

α-Aminooxy GalNAc-Texas Red C_{18}-Poly(MVK) (14). To a solution of **10** (6 mg, 0.09 mmol based on carbonyl number) in THF (5 mL) and H_2O (2 mL) was added **4α** (40 mg, 0.170 mmol), Texas Red hydrazide (5 mg, 8 μmol), and acetic acid (5 μL). The reaction mixture was stirred for 24 h at 95 °C, allowed to cool to room temp, and concentrated in vacuo. The resulting solid was dissolved in H_2O (7 mL) and heated to reflux for 48 h. The reaction mixture was cooled to room temp, dialyzed in H_2O, and lyophilized to give **14** (21 mg, 77% of carbonyls reacted) as a fluffy dark-red solid. IR (KBr): 3434, 1658, 1641, 1381, 1005, 557, 463 cm^{-1}. ^{1}H NMR (400 MHz, D_2O, δ/ppm, see Figure SI-15); GPC (H_2O eluent, polysaccharide standard), M_w = 30.9 × 10^3 Da, PDI = 2.56.

ACVA-PFP Ester (15). To a solution of 4,4′-azobis(4-cyanovaleric acid) (500 mg, 1.78 mmol) in CH_2Cl_2 (15 mL) was added *N*,*N*-diisopropylethylamine (745 μL, 4.28 mmol) and pentafluorophenyl trifluoroacetate (740 μL, 4.29 mmol). The solution was stirred at room temp for 6 h and evaporated to dryness. The resulting oil was purified by silica gel chromatography (8:1 hexanes/ethyl acetate) to afford **15** as mixture of isomers (274 mg, 25%). IR (thin film): 1796, 1514, 1390, 1296, 1094, 1052, 992 cm^{-1}. ^{1}H NMR (400 MHz, $CDCl_3$): δ 1.72 (s, 3 H), 1.85 (s, 6 H), 2.48−2.64 (m, 3 H), 2.65−2.72 (m, 3 H), 2.74−2.88 (m, 3 H), 2.92−3.04 (m, 3 H). ^{13}C NMR (100 MHz, $CDCl_3$): δ 23.66, 23.88, 28.23, 28.32, 32.69, 32.75, 71.60, 71.73, 116.99, 136.85, 138.50, 139.90, 141.75, 167.40. HRMS(FAB): Calcd for $C_{24}H_{15}F_{10}N_4O_4$ $[M+H]^+$, 613.0928; found, 613.0933.

Polymer (17). To a solution of dipalmitoylphosphatidylethanolamine (DPPE) (25 mg, 0.036 mmol) in MeOH (1 mL) and $CHCl_3$ (3 mL) was added *N*,*N*-diisopropylethylamine (10 μL, 0.072 mmol) and **15** (10 mg, 0.016 mmol). The solution was stirred at room temp for 2 h and evaporated to dryness. Anhydrous toluene (0.5 mL) and MVK (140 μL, 1.70 mmol) were added to the resulting oil. The reaction mixture was stirred for 72 h at 95 °C after degassing by four freeze−pump−thaw cycles. The reaction mixture was allowed to cool to room temp, diluted with *p*-dioxane (5 mL), and then added dropwise to excess diethyl ether (1 L) with vigorous stirring. The precipitate was filtered, washed with diethyl ether, and dried in vacuo overnight to afford **17** as a white solid (16 mg). IR (thin film): 2926, 1709, 1426, 1356, 1160, 1115, 734 cm^{-1}. ^{1}H NMR (400 MHz, $CDCl_3$, δ/ppm, see Figure SI-16); GPC (THF eluent, polystyrene standard), M_w = 11.8 × 10^3 Da, PDI = 1.31. Anal. Calcd for $(C_4H_6O)_n$: C, 68.54; H, 8.63. Found C, 69.32; H, 8.50.

GalNAc-Conjugated Polymer (18). To a solution of **17** (1.2 mg, 0.017 mmol based on carbonyl number) in THF (5 mL) and H_2O (2 mL) was added **4α** (10 mg, 0.042 mmol), Texas Red hydrazide (1.0 mg, 1.5 μmol), and acetic acid (5 μL). The reaction mixture was stirred for 24 h at 95 °C, allowed to cool to room temp and concentrated *in vacuo*. The resulting solid was dissolved in H_2O (7 mL) and heated to reflux for 48 h. The reaction mixture was cooled to room temp, dialyzed in H_2O, and lyophilized to give **18** (7 mg, 75% of carbonyls reacted) as a fluffy dark-red solid. IR (KBr): 3450, 1641, 1631, 1378, 1015, 569, 463 cm^{-1}. ^{1}H NMR (400 MHz, D_2O, δ/ppm, see Figure SI-17); GPC (H_2O eluent, polysaccharide standard), M_w = 65.7 × 10^3 Da, PDI = 1.30.

GalNAc-Conjugated Polymer (19). To a solution of **17** (1.2 mg, 0.017 mmol based on carbonyl number) in THF (5 mL) and H_2O (2 mL) was added ***4β*** (10 mg, 0.042 mmol), Texas Red hydrazide (1.0 mg, 1.5 μmol), and acetic acid (5 μL). The reaction mixture was stirred for 24 h at 95 °C, allowed to cool to room temp, and concentrated in vacuo. The resulting solid was dissolved in H_2O (7 mL) and heated to reflux for 48 h. The reaction mixture was cooled to room temp, dialyzed in H_2O, and lyophilized to give **19** (5 mg, 70% of carbonyls reacted) as a fluffy dark-red solid. IR (KBr): 3439, 1665, 1360, 1108, 1060, 963, 842 cm^{-1}. ^1H NMR (400 MHz, D_2O, δ/ppm, see Figure SI-18); GPC (H_2O eluent, polysaccharide standard), $M_w = 56.4 \times 10^3$ Da, PDI = 2.47.

LacNAc-Conjugated Polymer (20). To a solution of **17** (2.1 mg, 0.029 mmol based on carbonyl number) in THF (5 mL) and H_2O (2 mL) was added β-aminooxy-*N*-acetyl-lactosamine (17 mg, 0.043 mmol), Texas Red hydrazide (1.0 mg, 1.5 μmol), and acetic acid (5 μL). The reaction mixture was stirred for 24 h at 95 °C, allowed to cool to room temp, and concentrated in vacuo. The resulting solid was dissolved in H_2O (7 mL) and heated to reflux for 48 h. The reaction mixture was cooled to room temp, dialyzed in H_2O, and lyophilized to give **20** (5 mg, 60% of carbonyls reacted) as a fluffy dark-red solid. IR (KBr): 3250, 2950, 1560, 1400, 1350, 1010, 980 cm^{-1}. ^1H NMR (400 MHz, D_2O, δ/ppm, see Figure SI-19); GPC (H_2O eluent, polysaccharide standard), $M_w = 73.8 \times 10^3$ Da, PDI = 2.03.

Supported Lipid Bilayers.[19] Lipids were mixed in $CHCl_3$ followed by evaporation of the organic solvent. The dried lipid films were hydrated in distilled, deionized water (2 mg lipid per mL) at 4 °C for 12 h. Small unilamellar vesicles (SUVs) were formed by repeated extrusion of the lipid suspension at 50 °C through polycarbonate filters with 100 nm pores using a Lipex extruder. SUVs were mixed with phosphate buffered saline (PBS) solution to a final concentration of 0.4 mg lipid/mL solution and then incubated with clean glass cover slips for several minutes. Rupture of the vesicles with the substrate formed a continuous lipid bilayer, which was kept in PBS. The lipid membrane composition for experiments involving mucin mimic polymer incorporation was 95% mole % DOPC (1,2-dioleoylsn-glycero-3-phosphocholine) and 5% DOTAP (1,2-dioleoyl-3-trimethylammonium-propane) (Avanti Polar Lipids, Alabaster, AL). For determination of lipid mobility, lipid membranes were composed of 94% DOPC, 5.5% DOTAP, and 0.5% Texas Red DHPE (Texas Red 1,2-dihexadecanoyl-*sn*-glycero-3-phosphoethanolamine) (Invitrogen, Carlsbad, CA).

Microscopy and Florescence Recovery after Photobleaching. Images were obtained at room temp using a Nikon TE300 inverted fluorescence microscope with a Hamamatsu ORCA 2 charge-coupled device camera and SIMPLE PCI acquisition software. Illumination was provided via a mercury arc lamp. The density of Texas Red-labeled mucin mimetic polymers was determined from fluorescence intensity values by comparison with the fluorescence from supported lipid bilayers with known densities of Texas Red-labeled lipids, under identical optical conditions. The relative densities of bound lectins were determined by measuring the fluorescence intensity of the lectins' FITC label; relative binding affinities were determined by normalizing the FITC intensity to the intensity of the Texas Red label of the incorporated polymers to account for variations in polymer density.

Molecular mobility was measured by examining fluorescence recovery after photobleaching (FRAP). Fluorescent probes in a region defined by a partially closed aperture were bleached by intense illumination for 10 s. Images were captured as mobile bleached and nonbleached fluorescent probes diffused among each other and were analyzed using custom software written with MATLAB (Mathworks, Natick, MA), described below, to extract the diffusion coefficient of the molecules. The local concentration (C) of molecules with unbleached fluorophores is proportional to the fluorescence intensity (I) at each pixel. (The background intensity, due mainly to read-out noise from the CCD camera, was measured and subtracted from each image, and the density of fluorophores is low enough, by over a factor of 10, that nonlinear self-quenching effects are negligible. Thus, C is proportional to I.) The diffusing molecules were assumed to obey the statistical relations governing two-dimensional random walks, one of the consequences of which is that over a time increment $\Delta t = \Delta x^2/2D$, where Δx is the pixel size (the unit of our discrete measurement of C) and D is the diffusion coefficient; the concentration at a given pixel becomes equal to the average of the concentration at its nearest neighbor pixels. To extract D from a pair of fluorescence images, I_1 and I_2, separated in time by an amount Δt, the initial image (I_1) was acquired and then subjected to a series of nearest-neighbor averaging steps. At each step (j), the resulting image (I_1') was compared with I_2, and their deviation was calculated: $\chi^2(j) = \Sigma((I_1' - I_2)^2)$. The j that yields the minimal χ^2 revealed the number of increments of $\Delta t = \Delta x^2/2D$ that occur in the time interval between the two images, that is, $j\Delta x^2/(2D) = \Delta t$, or $D = j\Delta x^2/(2\Delta t)$, providing D in terms of experimental parameters. Notably, this method does not rely on assumptions about the shape of the bleached spot or on precise measurements of the bleaching time, being sensitive only to differences between the two recorded images. Several pairs of images were used to deduce the D values stated in the text; the uncertainty reported is the standard deviation.[28]

Acknowledgment. G.S.L. was supported by a postdoctoral fellowship from the Korea Science & Engineering Foundation (KOSEF). This research was supported by a grant to C.R.B. from the National Institutes of Health (Grant GM59907) and The Director, Office of Science, Office of Basic Energy Sciences, Division of Materials and Engineering, and the Office of Energy Biosciences of the U.S. Department of Energy under Contract No. DE-AC03-76SF00098. We thank Dr. Marian Snauko for helpful discussions and assistance with polymer characterization and Chris Harland for assistance with imaging bilayers.

Supporting Information Available: Synthetic procedures for compounds **1**−**3** and **9**; IR, ^1H NMR, and GPC spectral data for compounds **1**−**3**, **5**−**7**; TEM image of **3**; ^1H NMR spectral data for compounds **10**−**14** and **17**−**20**; binding of FITC-HPA to supported bilayer. This material is available free of charge via the Internet at http://pubs.acs.org.

JA067819I

(28) Berg, H. C. *Random Walks in Biology;* Princeton University Press: Princeton, NJ, 1993; Chapter 1.